Performance validation of the first arm of FALSTAFF: ^{252}Cf and ^{235}U fission fragment characterisation

D. Doré[1], E. Berthoumieux[1], Q. Deshayes[1], L. Thulliez[1], P. Legou[1], M. Combet[1], M. Kebbiri[1], A. Marcel[1], J-Ph. Mols[1], M.O. Frégeau[2], S. Herlant[2], X. Ledoux[2], J. Pancin[2)], S. Oberstedt[3]

[1] Irfu, CEA, Université Paris-Saclay, Gif-sur-Yvette, F-91191, France
[2] GANIL, F-14050 Caen, France
[3] European Commission, Joint Research Centre, Directorate G Nuclear Safety and Security, Unit G.2, Retieseweg 111, 2440 Geel, Belgium

Abstract. The renewed interest for the study of nuclear fission is mainly motivated by the development of GEN-IV reactor concepts, mostly foreseen to operate in the fast neutron energy domain. To support this development, new high-quality nuclear data are needed. In this context, a new experimental setup, the FALSTAFF spectrometer, dedicated to the study of nuclear fission is under development. Employing the double-velocity (2V) and energy-velocity (EV) methods, the fission fragment mass before and after neutron evaporation will be deduced and the correlation between prompt neutron multiplicity and fragment mass will be determined. The first arm of the spectrometer is achieved. It is composed of two SED-MWPC detectors (a combination of a foil to produce secondary electrons and a Multi-Wire Proportional Chamber to detect them) and an axial ionization chamber. The SED-MWPC give access to the velocity (V) via time-of-flight and position measurements. The ionization chamber measures the fragment kinetic energy (E) and the energy loss profile. Preliminary results for spontaneous fission of ^{252}Cf and from the thermal-neutron induced fission experiment on ^{235}U, performed at the Orphée reactor (CEA-Saclay, France), are presented.

1 Introduction

Nowadays the fission process still presents a great interest from both theoretical and experimental point of view. New developments on microscopic calculations and the future generation of nuclear reactors are among the main motivations for new experimental programs devoted to the study of nuclear fission. The FALSTAFF project [1-2] aims at providing highly constrained data to improve significantly the description of the fission process. The goal is to determine the neutron multiplicity as a function of the fragment characteristics (pre-neutron mass and kinetic energy) in neutron-induced fission of specific actinides in the MeV range. This experiment is particularly rich as it allows accessing numerous aspects of fission, e.g. the deformation at scission, the influence of single-particle

structure in neutron-rich isotopes, the dissipated energy and the energy partition between the two fragments. In order to maintain a fair detection efficiency, neutrons are not measured, but their multiplicity is deduced in average from the measured fragment masses before and after their evaporation.

Based on time-of-flight and residual energy technique, the FALSTAFF setup will consist of two arms allowing the simultaneous measurement of the complementary fragment velocities and energies. The combined measurements of velocities and energies provide information on the mass of the fragments before (pre-) and after (post-) the neutron evaporation. The 2V method (measurement of both fragment velocities in coincidence) gives access to the pre-neutron mass. This method is meaningful only when the mass of the fissioning system is known, namely for incident neutron energies below the threshold of the second chance fission channel opening ($E_n < 5.5$ MeV). The limitation of this technique is linked to the intrinsic velocity dispersion brought by neutron evaporation, which degrades the mass resolution. The post-neutron mass is obtained with the EV (energy-velocity) method. The average prompt neutron multiplicity as a function of the fragment mass distribution may then be deduced from the event-wise difference between pre- and post-neutron masses.

The experimental setup will be described in section 2. Results for the spontaneous fission of ^{252}Cf and the thermal neutron-induced fission of ^{235}U will be presented in section 3 and 4 respectively.

2 Experimental setup

A sketch of the FALSTAFF setup is shown in Fig. 1. Each arm is composed of two ToF detectors (SeD Start and SeD Stop) and an axial ionization chamber. The necessary timing and position resolutions for the ToF detectors are obtained by using a combination of an emissive foil and a MWPC detector. Ionization chambers will be placed behind the stop detectors to measure the fragment residual energies. In addition, the light-fragment nuclear charge could be estimated thanks to the fragment energy-loss profile in the ionization chamber.

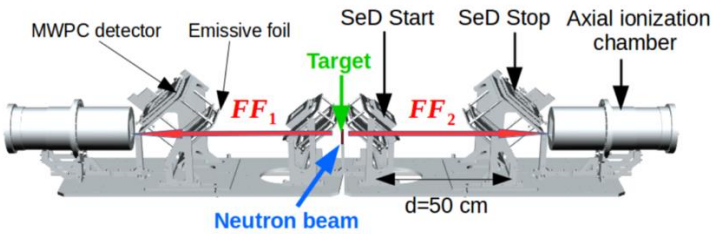

Fig. 1. Sketch of the FALSTAFF spectrometer (see text for details).

2.1 The time-of-flight (ToF) detectors

For the ToF detectors [3-5] an aluminized Mylar foil of 0.5 µm thickness, inclined at 45 deg with respect to the horizontal direction and polarized at -10 kV, is placed along the path of the fission fragments. A grounded grid placed at 1 cm from the emissive foil generates a high electric field close to the foil. The secondary electrons produced by the ion

crossing the Mylar foil are then accelerated to 10 keV and fly towards the MWPC detector. The accelerated electrons pass through the MWPC entrance foil (made from 0.9 μm aluminized Mylar) with 70% efficiency [5]. They create ionization electrons inside the gas which are then amplified while drifting towards the cathode. The amplification takes place over the whole drift path due to the low pressure of the gas (0.6-0.8 kPa). The time signal is then read from the wire plane by a fast amplifier. The spatial information is taken from the charge induced on a 2D pixelized cathode for the stop detector while the start detector is made of three perpendicular wire planes from which two planes are used to obtain the position.

Timing and spatial resolutions of each ToF detectors were measured with a dedicated setup. Values of 100-120 ps and 1-2 mm were obtained for the time and spatial resolutions respectively.

2.2 Axial ionization chamber

The choice of an axial field for the ionization chamber was motivated by the possibility to reconstruct the energy loss profile by detecting the number of electrons as a function of the time of arrival on the anode. Moreover, the dead zones are minimized for this type of ionization chamber.

The cylindrical axial ionization chamber [3] has an outside effective diameter of 440 mm and a length of 400 mm. The cathode is the detector entrance window separated from the anode by a distance of 395 mm. A potential of -8 kV is applied to the cathode, while the anode is the readout electrode. The entrance window is a Mylar foil, 0.9 μm thick and with a diameter of 232 mm. To polarize the Mylar foil and to ensure a good electrical conductivity, 50 nm of aluminum are deposited on each side. In order to avoid strong mechanical tension, the entrance window is supported by a grid of 12 nylon wires, 6 vertical and 6 horizontal. These wires have a diameter of 350 μm. The electric field uniformity is assured by 38 aluminum rings, 270 mm in diameter, spaced out by 10 mm and interconnected by a 10 MOhm resistance allowing to maintain a uniform field along the chamber.

A Frisch grid is installed in front of the anode to ensure the shielding from the influence of the charges moving in the ionization region. The main part of the electronic signal on the anode is induced by electrons after they have crossed the grid. The Frisch grid is made up of 68 tungsten wires, 170 μm in diameter and spaced out by 4 mm. The ionizing gas is isobutane at a pressure between 2.7 and 4.0 kPa flowing at 0.5 Ln/ h.

The energy resolution measured with an alpha source (^{241}Am) was estimated to 3.9 %. A better resolution is expected for fragments since the signal amplitude is larger.

2.2 Acquisition systems

Two independent acquisition systems (DAQ) are used to collect the data:

1- the cathode pad/strips signals from the start and stop detectors are digitized using the GET acquisition system [6] on a μTCA crate,

2- all others signals (timing information from start and stop detectors, anode and grid signal from the axial ionization chamber) are recorded by using the standard GANIL acquisition based on a VME crate.

For the start and stop detectors the anode signals are digitized by using a Matacq card [7] having a 2 GHz sampling rate. The anode and grid signals from the ionization chamber are digitized by using a CAEN V1724 card having 100 MHz sampling rate.

3 Results for the spontaneous fission of ^{252}Cf

A ^{252}Cf source was placed behind a collimator at 10 cm in front of the emissive foil of the start detector. The trigger was constructed from the coincidence of start and stop detector signals. The time distribution is calibrated by using an alpha source. Geant4 simulations were used to calibrate the residual fragment energy distribution.

In Fig. 2 the experimental velocity, energy and mass distributions are shown in red. They are compared to simulated distributions. These simulations were performed with GEANT4. Two different event generators were used: FIFRELIN [8] in green dotted line and GEF [9] in blue dashed line. The measured resolutions for the position and the time (σ(t)= 120 ps; σ(pos) = 2 mm) and the expected one for the energy (dE/E= 1%) are taken into account in the simulations. It has previously been shown [1-3] that these resolutions allow to reproduce the correlation between neutron multiplicity and pre-evaporation fragment mass well enough to study the evolution of the correlation as a function of the excitation energy.

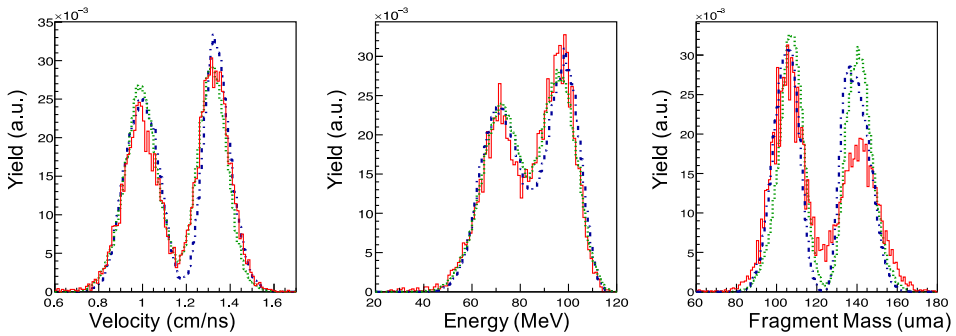

Fig. 2. Velocity (left panel), energy (middle panel) and post-evaporation fragment mass (right panel) distributions for FALSTAFF (red curve) are compared to GEANT4 simulations with two different event generators: FIFRELIN (green dotted curve) and GEF (blue dashedcurve).

The simulated velocity and energy distributions show a rather good agreement with experimental distributions. One observes that the main differences for the fragment mass distribution are the width of the experimental distribution for heavy fragments and the lack of heavy fragments compared to light ones. The discrepancy for the width could be due to a difference in simulated and experimental resolutions although this is neither visible in the velocity nor in the energy distributions. The lack of heavy fragments is not visible for all data taking. This fact comes from the signal-to-noise ratio which varied from one run to another. The signals from the heavy fragments being small, some good events were rejected due to the signal being below the trigger threshold. A comparison (Fig. 3) with the experimental mass distributions from SPIDER [10] and VERDI [11], which are 2V-2E spectrometers, leads to same conclusion and is depicted in Fig. 3.

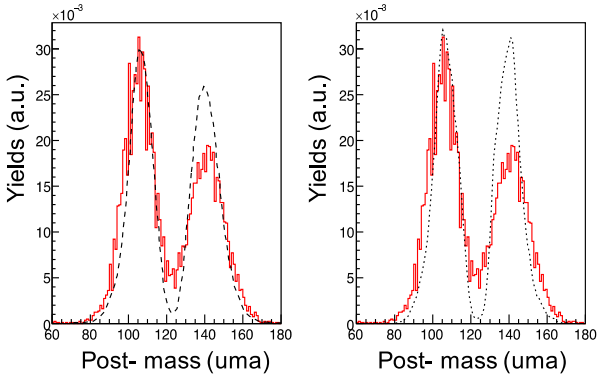

Fig. 3. ^{252}Cf FALSTAFF fragment mass distribution (red curve) is compared to VERDI (left panel) and SPIDER (right panel) results.

4 Results from the thermal neutron-induced fission of ^{235}U

An experiment was performed in 2018 at the Orphée reactor to test one arm of the FALSTAFF spectrometer in real conditions, by measuring the post-neutron emission mass distribution of ^{235}U thermal neutron induced fission. A neutron flux of 7.4E+06 n/cm^2/s was measured at the neutron beam entrance window of FALSTAFF. The experiment was performed with a ^{235}U target of 6.4 µg/cm2 and a restricted FALSTAFF geometrical efficiency of 0.4 %. Velocity and corrected energy distributions obtained for this experiment are presented in Fig. 4. Simulated distributions are also shown.
The velocity distribution is slightly distorted for the light fragment peak compared to simulations. This was also observed for the ^{252}Cf(sf) and has to be investigated. In the distributions, the loss of heavy fragment is seen again. This problem could be solved by amplifying the signal earlier in the electronic chain.

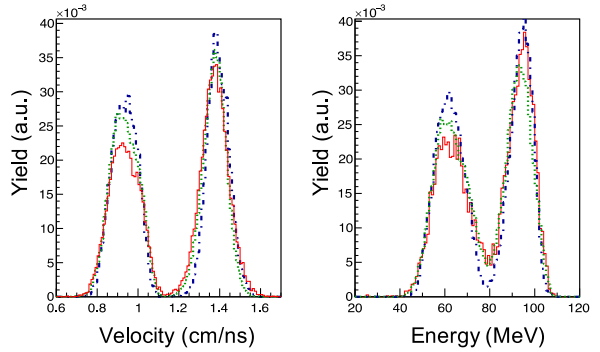

Fig. 4. ^{235}U FALSTAFF velocity and energy distribution (red curve) are compared to GEANT4 simulations with two different event generators: FIFRELIN (green dotted curve) and GEF (blue dashed curve).

5 Outlook/Conclusion

The recent results obtained with the first arm of FALSTAFF have been presented. For the ToF detectors, the requested performances are in reach, although the operation turned out to

be unstable. For the ionization chamber, the electronic chain and the Frisch grid have to be improved in order to reach an energy resolution of 1%.

The operation of the spectrometer in experimental conditions using a neutron beam showed no additional performance degradation with respect to the source measurement. After an optimization phase, the next step of the project will be the construction of the second arm of the spectrometer to achieve the full 2V-EV measurement of fission fragments.

Acknowledgments

This work was partially supported by CEA, NEEDS, P2IO and within the Seventh Framework Programme through CHANDA (EURATOM contract no. FP7-Fission-2013-605203). The authors thank the team members of the Orphée reactor for their support and O. Litaize et O. Serot for providing results of FIFRELIN.

References

1. D. Doré et al., EPJ Web of Conference **42** (2013) 01001.
2. D. Doré et al., Nuclear Data Sheets **119** (2014) 346-348.
3. L. Thulliez, Ph.D. Thesis, Université Paris-Saclay, 25 Sept. 2017.
4. L. Thulliez et al., EPJ Web of Conferences **146** 04028 (2017).
5. J. Pancin et al. J. Instrum., **4** (2009) P12012.
6. E. Pollacco et al., NIM A **887** (2018) 81-93.
7. D. Breton, E. Delagnes, IEEE Nuclear Science Symposium, Medical Imaging Conference, and 15th International Room Temperature Semiconductor Detector Workshop, San Diego, United States, Oct. 2006, IEEE, 2, pp.990-995, 2006.
8. K.H. Schmidt et al., Technical report, JEFF Report 24, 2014.
9. A. Litaize et al., Phys. Rev. C **82** (2010) 054616.
10. K. Meierbachtol et al., NIM A**788** (2015) 59-66.
11. M.O Frégeau et al., NIM A**817** (2016) 35-41.
12. K. Jansson et al., Eur. Phys. J. A **54** (2018) 114**.**